Tectonics

RESEARCH ARTICLE
10.1029/2020TC006188

Slab Detachment, Mantle Flow, and Crustal Collision in Eastern Sicily (Southern Italy): Implications on Mount Etna Volcanism

G. Barreca[1,2], S. Branca[3], R. A. Corsaro[3], L. Scarfì[3], F. Cannavò[3], M. Aloisi[3], C. Monaco[1,2,3], and C. Faccenna[4,5]

[1]Department of Biological, Geological and Environment Sciences, University of Catania, Catania, Italy, [2]CRUST—Interuniversity Center for the 3D Seismotectonic analysis with territorial applications, c/o DiSPUTer - Ud'A, Campus Universitario di Madonna delle Piane, Chieti, Italy, [3]Istituto Nazionale di Geofisica e Vulcanologia (INGV-OE), Catania, Italy, [4]Department of Geological Sciences, Jackson School of Geosciences, Austin, TX, USA, [5]Department of Sciences, Roma Tre University, Rome, Italy

Key Points:
- The crust below the volcano is currently involved in deep-seated contraction as result of subduction cessation and collision onset
- Increasing in explosiveness, lateral eruptions and changes in lava composition are interpreted as controlled by deep-seated crustal shortening beneath the volcano
- According to the reconstructed geodynamics, anomalies in the late evolution of Mount Etna could indicate a declining stage for the volcano

Correspondence to:
G. Barreca,
g.barreca@unict.it

Citation:
Barreca, G., Branca, S., Corsaro, R. A., Scarfì, L., Cannavò, F., Aloisi, M., et al. (2020). Slab detachment, mantle flow, and crustal collision in eastern Sicily (southern Italy): Implications on Mount Etna volcanism. *Tectonics*, *39*, e2020TC006188. https://doi.org/10.1029/2020TC006188

Received 4 MAR 2020
Accepted 27 JUL 2020
Accepted article online 4 AUG 2020

Abstract New data and interpretations of the geodynamics of eastern Sicily point to deep crustal shortening taking place in the area. Reconstructions of the lithospheric system, seismicity distribution, and stress state in the crust indicate that deformation is expressed by a large thrust-ramp cutting through the entire lower plate. The tectonic structure is propagating directly beneath the Mount Etna volcano, one of the few active volcanoes in Europe. Geostructural interpretation of tomographic sections allows for interpretations of the compressional structure as originating in response to trench-parallel breakoff of the Ionian slab. Following the simple assumption that if a slab retreats, it must either be compensated or alternatively pushed by the fore-arc mantle, we argue that the opening of a gateway in the slab has encouraged the fore-arc mantle to flow toward the Mount Etna region. Mantle mobilization has had a twofold influence on both magmatic source mixing and the inception of underplating processes beneath the Mount Etna. A shortening prevailing over extension in the crust below the volcano seems to have a significant impact on the dynamics of the Mount Etna volcanic system, which manifested through anomalous signals over the last thousands of years. Since a tectonic inversion of previous dilatational magma pathways is expected in such a converging setting, the documented variations are believed to be consistent with a volcano experiencing a declining phase. Comparison with other extinct volcanic systems in the southern Tyrrhenian margin, lying atop a detached slab and involved in contraction, provides insights into the evolution of Mount Etna.

1. Introduction

Mount Etna is a majestic volcano that, rising to a height of over 3 km above sea level (a.s.l.), dominates the skyline of the central Mediterranean. Formed 500 ka ago along a diverging zone in the framework of the Africa-Europe plate convergence, its origin is currently best explained through a deep and vertical tearing in the lithosphere caused by the dynamics of slab retreat at the southern edge of the Ionian/Calabrian subduction zone (Doglioni et al., 2001; Gvirtzman & Nur, 1999; Hirn et al., 1997; Figure 1a). Following the slab edge deformation, the passive upwelling of asthenospheric material alongside the tearing structure (Figure 1b) gave rise to mantle melting because of adiabatic decompression (Gvirtzman & Nur, 1999). The growth of a subduction edge volcano is considered the last episode of long-lasting intraplate magmatism affecting Eastern Sicily (Barberi et al., 1974; Pedley et al., 1993). From the late Cretaceous onward, tholeiitic to Na-alkaline lava products were emitted by fissure-type volcanism along the eastern sector of the Hyblean foreland, and later they accumulated to the north mainly at the foreland-foredeep transition domain (Figure 1c), where the earliest Etna volcanic products were also emplaced (Branca et al., 2008; Schmincke et al., 1997). Subcrustal transtensional faulting and associated fracturing then facilitated magma ascent through the lithosphere along the Ionian coast of Sicily (Hirn et al., 1997; Monaco et al., 1997). Here, volcanic products have accumulated above a Neogene-Quaternary sedimentary clayey basement to form the Mount Etna composite stratovolcano.

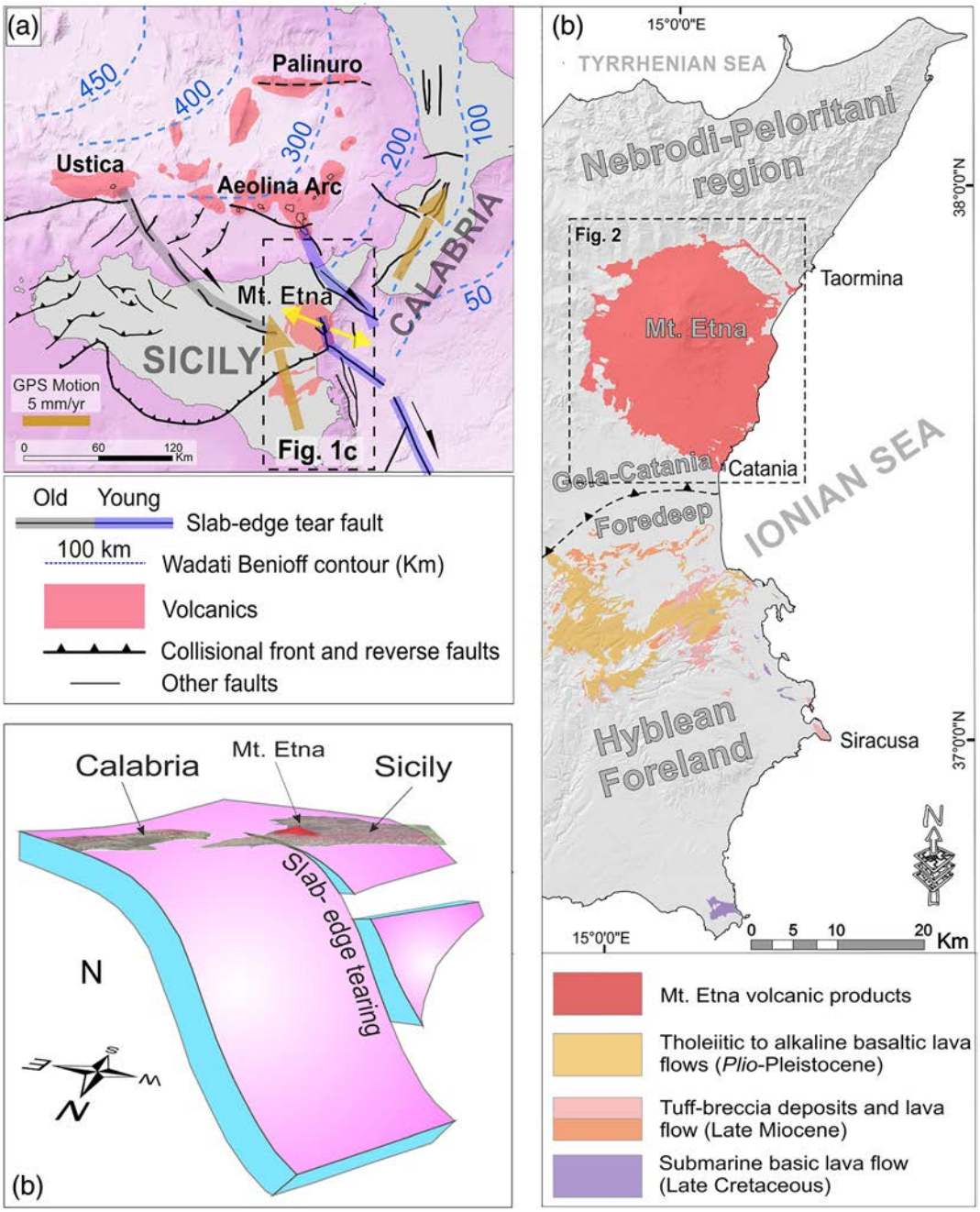

Figure 1. Mount Etna in the geodynamic framework of the Central Mediterranean. (a) Mount Etna lies atop the modern slab-edge tear faulting at the SW margin of the Ionian subduction system. Orange arrows indicate diverging geodetic velocities (see D'Agostino & Selvaggi, 2004; Mastrolembo Ventura et al., 2014; Ward, 1994) measured in the lower plate of the collisional system. Decomposing of the diverging vectors resolves a WNW-ESE trending extension along the E-Sicily/Western Ionian Basin domain (small yellow arrows). (b) Extension at slab edge allowed magma ascent and the formation of Mount Etna volcano, which is considered the last episode of intraplate magmatism affecting Eastern Sicily since the Cretaceous (c). Bathymetric data in (a) and topography in (c) were extracted from the Emodnet bathymetry (http://www.emodnet-bathymetry.eu) and from the SRTM (Shuttle Radar Topography Mission) 30 plus topography (http://topex.ucsd.edu/WWW_html/srtm30_plus.html), respectively. Major faults in (a) are from Barreca et al. (2014, 2016), Cultrera et al., 2016, 2017), Barreca et al. (2019), and Gutscher et al. (2016). Volcanic outcrops in (c) were extracted from Lentini and Carbone (2014).

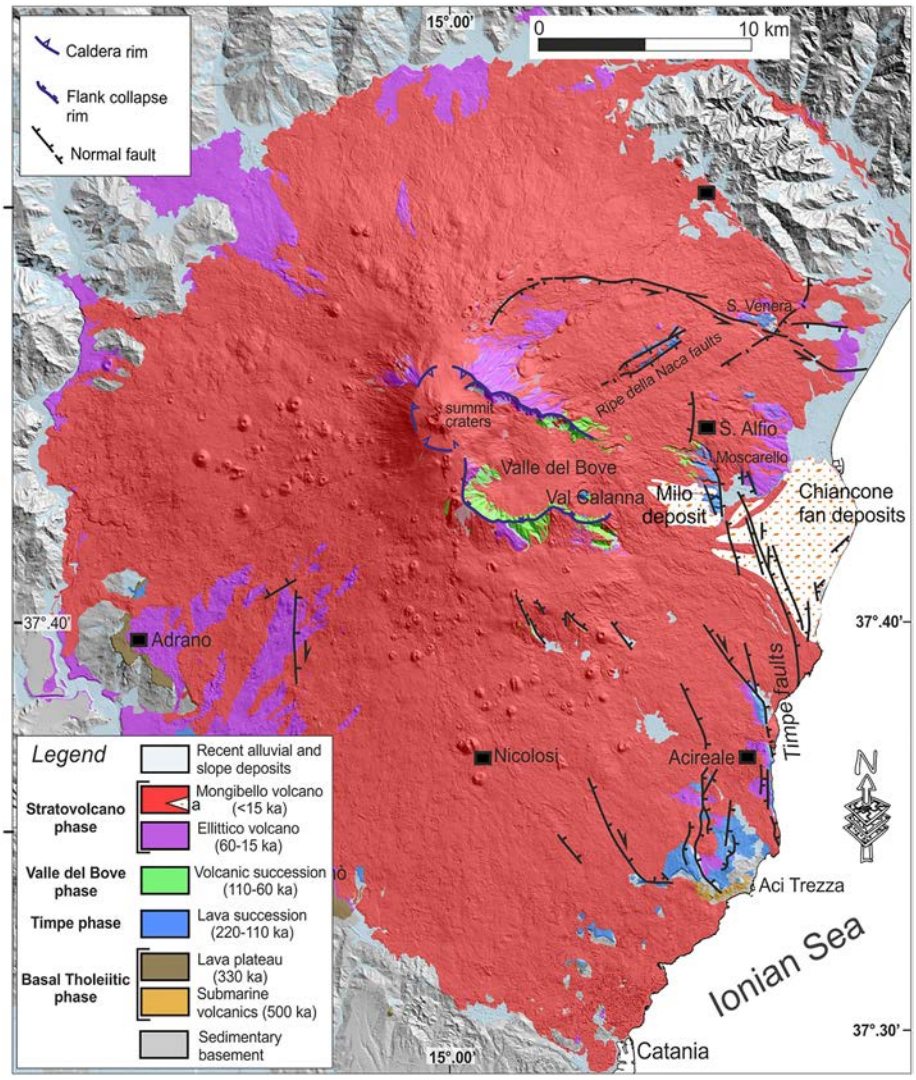

Figure 2. Main volcanic phases reconstructed for the Mount Etna volcano (Branca et al., 2008).

Several phases in the evolution of the volcano have been unraveled by extensive field mapping, radiometric dating and historical records (Branca, Coltelli, & Groppelli, 2011; Branca, Coltelli, Groppelli, & Lentini, 2011; De Beni et al., 2011; Gillot et al., 1994; Figure 2). Age constraints and the type of volcanic products revealed that the early phase of Mount Etna (Basal Tholeiitic phase, 500–330 ka, Figure 2) started in a submarine environment (i.e., the Ionian Sea) and continued subaerial since 330 ka, when the sector where Mount Etna was created was uplifted by regional tectonics (Di Stefano & Branca, 2002). During this stage, fissure-type eruptions emitted lava flows of tholeiitic composition similar to the Pliocene-lower Pleistocene volcanism of the northern border of the Hyblean foreland (Figure 1c), which accumulated to form thin lava plateaus (Branca, Coltelli, & Groppelli, 2011). After a hiatus of about 100 kyr, volcanic activity resumed along the Ionian coastal domain, forming a gently sloping lava shield volcano (Timpe Phase, 220–110 ka, Figure 2) and, 130 ka ago, it began to migrate westward (De Beni et al., 2011; Gillot et al., 1994). Mount Etna began to grow rapidly, becoming a central-type volcano with the formation of many polygenetic centers (Valle del Bove and Stratovolcano phases, Figure 2), which were active between 110 and 15 ka (De Beni et al., 2011). Among these, the Ellittico reached a maximum elevation of about 3.6 km a.s.l. (about 300 m higher than at present) until its summit collapsed through huge Plinian eruptions about 15 ka (Branca, Coltelli, Groppelli, & Lentini, 2011; Coltelli et al., 2000; Del Carlo et al., 2017).

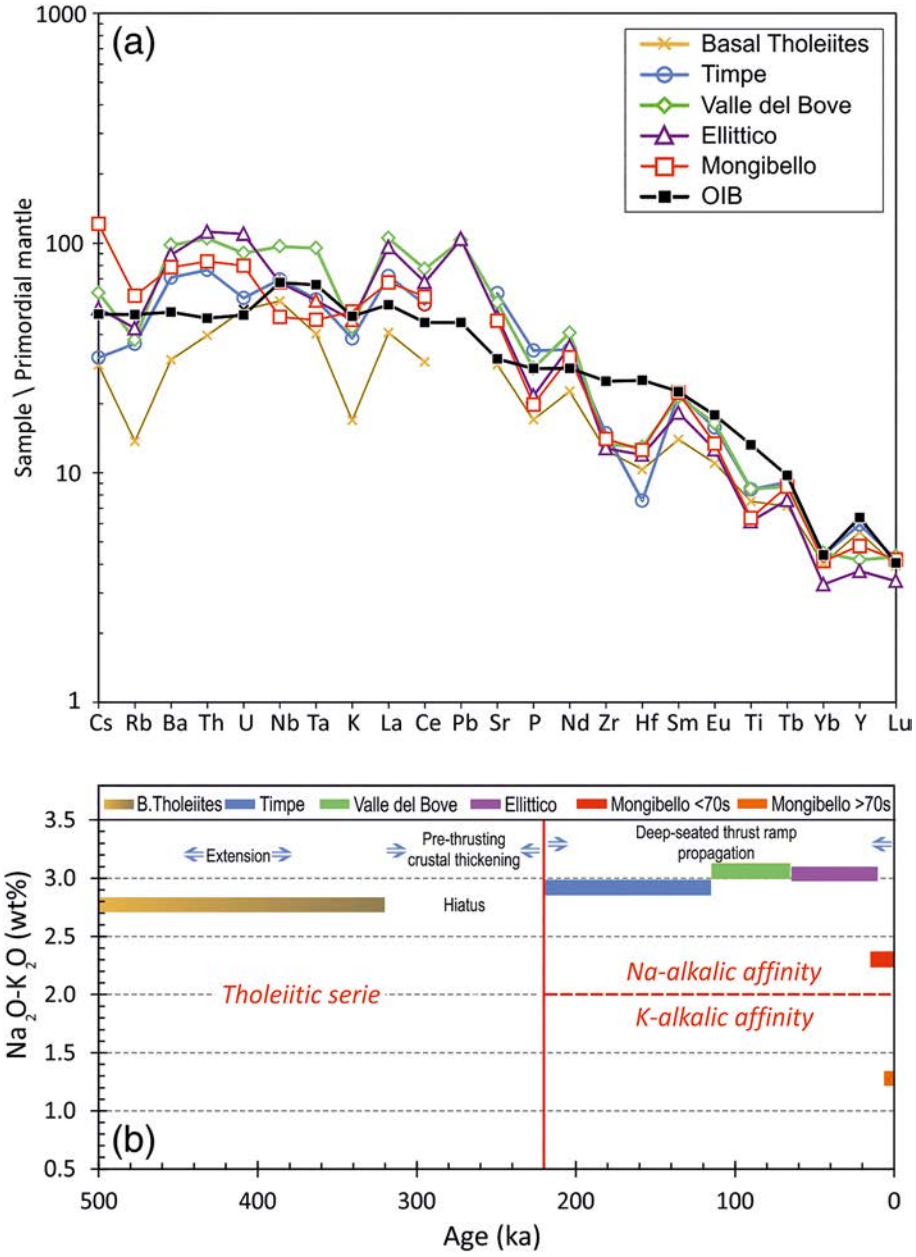

Figure 3. Geochemistry at Mount Etna. (a) Incompatible element patterns of Etnean mafic rocks (analyses from Corsaro & Pompilio, 2004) normalized to primordial mantle (McDonough & Sun, 1995). Average OIB is shown for comparison (McDonough & Sun, 1995). The composition of Etnean magmas is mostly OIB-type (see text for details). (b) Compositional variation of Etnean volcanic sequence over the time. Tholeiites range from about 500 to 320 ka. After a ~100 kyr hiatus, volcanism restarted with the eruption of a Na-alkalic magma from 220 ka up to the 1970s. Later and up to now, the erupted products shifted to K-alkalic affinity. Analyses of major and trace elements in bulk rocks of Mount Etna are a collection from different laboratories summarized in Corsaro and Pompilio (2004) (see this paper for details). The threshold Na_2O-$K_2O \geq 2$ (%wt) separates the field of Etnean rocks with Na and K-alkalic affinity, according to Le Maitre (2002). Arrows indicate the inferred tectonic regime acting at the time of eruptive events emplacement.

Even if Etnean magmas show a geochemical signature of ocean island basalt (OIB, Armienti et al., 1989; Tanguy et al., 1997), it is well known that alkaline lavas show the imprint of subduction-related components (Armienti et al., 1989), such as the enrichment of fluid mobile elements like K, Rb, Cs, B, and radiogenic Sr (Armienti et al., 2004; Schiano et al., 2001; Tonarini et al., 2001). Other long-term compositional variations are observable in Etnean volcanic rocks (Armienti et al., 2013; Condomines et al., 1995; Di Renzo et al., 2019;

Marty et al., 1994; Tanguy, 1987; Tanguy et al., 1997; Viccaro et al., 2010). The oldest volcanic products are basalts of a subalkaline series (Basal Tholeiitic phase), which evolved since 220 ka to an alkaline series, ranging in composition from alkali-basalts to trachytes (Timpe to Stratovolcano phases). Alkaline magma with sodic affinity was erupted up to the 1970s; later, a potassic affinity became dominant and has remained stable until today (Corsaro & Pompilio, 2004; Peccerillo, 2017; Figure 3b).

To date, Mount Etna has been considered as a stand-alone volcanic system and its evolution has never been properly framed in the wider geodynamic context where the volcano is situated. Considering that significant variations in volcanism throughout southern Italy have been influenced by the evolving geodynamic setting (see Peccerillo, 2005, and references therein), in this work, we have retraced the entire geological history of the volcano from a critical perspective and analyzed some significant changes in magma composition and in the eruptive style in light of the geodynamics of the region. Largely based on the reconstruction of the lithospheric system beneath Eastern Sicily, we propose new interpretations of (1) the origin of the tectonic forces beneath and around the volcano and (2) the effects that this stress could have on the evolution of the volcano. The sharp increase in the number of flank and explosive eruptions in the last thousands of years, the changes of magma composition over time, as well as the current volcano-tectonic deformation pattern documented in the literature have been associated with a significant geodynamic reorganization in the area (Goes et al., 2004). According to a tectonic scenario where the volcano is involved in deep-seated contraction, the anomalies documented for the most recent phases of the volcano could be premonitory signals of volcanic decline.

1.1. Major Changes in Mount Etna's Evolution

The different phases in the evolution of Mount Etna have been marked by significant compositional variations of magmas (Corsaro & Pompilio, 2004, and references therein; Peccerillo, 2017, and references therein), in the eruptive style (Del Carlo et al., 2004), and in the emitted volume (Barreca, Branca, & Monaco, 2018; Branca & Ferrara, 2013) of volcanic products. In this section, we retrace the Mount Etna evolution focusing on major variations that have conditioned the geologic evolution of the volcano. The current state refers instead to the most recent stage of the volcano (Mongibello, last 15 ka) and particularly to the last thousands of years, when important variations in the eruptive style also occurred.

Variations in the geochemical signature of products emitted throughout the volcano's evolution have been discussed and interpreted with several theories, which are not detailed in this paper, but summarized in the literature (Corsaro & Pompilio, 2004; Peccerillo, 2017). The geochemical variations of Etna products are thought to be the result of magmatic processes occurring in the source region and/or in the crust beneath the volcano. For instance, the trace element pattern (Figure 3a) of Etnean magmas is close to the "Ocean Island Basalts" (OIB, McDonough & Sun, 1995). However, the rocks show a systematic enrichment of fluid mobile elements like K, Rb, Cs, B, and radiogenic Sr, suggesting that the typical OIB plume-related signature of Etnean magmas has been contaminated by subduction-related components in the mantle source (Armienti et al., 2004; Schiano et al., 2001; Tonarini et al., 2001). Other compositional variations occurred throughout the volcano's activity (Corsaro & Pompilio, 2004; Peccerillo, 2017). For example, the switch from subalkaline to alkaline primary magmas, which occurred after 220 ka, following the 100-ka hiatus of the volcanic activity, is generally explained considering two extreme hypotheses involving the mantle region. Some authors suggest that tholeiitic and alkaline magmas are generated from two or more distinct mantle sources (Chester et al., 1975; Condomines et al., 1982; Joron & Treuil, 1984), while for others (Tanguy, 1987; Tanguy et al., 1997) tholeiitic and alkaline magmas derive from a homogeneous source that may have undergone different degrees of partial melting, lower for alkaline rock (see Corsaro & Pompilio, 2004). Further compositional changes of magma composition took place in the crust mostly within the shallow volcanic plumbing system, where primary magmas differentiate, mainly for mixing and fractional crystallization at different depths (Corsaro & Pompilio, 2004, and references therein; Peccerillo, 2017, and references therein). The important role of fractional crystallization in controlling magma composition became evident during the Ellittico volcano stage (60–15 ka, Figure 2) when magma widely changed from alkali-basalt to trachyte (Nicotra & Viccaro, 2012). As regards the eruptive style, tephrastratigraphic studies revealed that Etna was characterized by effusive eruptions during much of its existence. Only episodic, small-medium magnitude eruptions, ranging from Strombolian to sub-Plinian events, and very rare Plinian eruptions, have occurred during the last 100 ka (Coltelli et al., 2000). However, the explosivity of Etna has significantly increased

since the last 4 ka (Del Carlo et al., 2004). The total number of flank and summit explosive eruptions (Branca, Coltelli, Groppelli, & Lentini, 2011; Del Carlo et al., 2004) of Mongibello volcano (last 15 ka, Figure 2) sharply increased during the past 4 ka. In this period, the average number of flank eruptions per year is 0.042, more than twice the 0.016 determined during the 11 ka before. At the same time, a very intense period of explosive summit activity started following the picritic sub-Plinian eruption of 3,930 ± 60 BP. Thereafter, the frequency and magnitude of explosive eruptions sharply increase up to 4 times higher than in the previous 8 ka, remaining constant until the present (Del Carlo et al., 2004). In the recent past, the volcano gave rise to explosive summit eruptions (unusual for a basaltic volcano) whose frequency has increased notably since the 1970s, and in the late 1990s, there were >200 of these paroxysmal episodes accompanied by abundant gas emission. These variations in the eruptive style may be related to magma compositional variation within a contaminated source region (see Schiano et al., 2001) and/or in the volcanic plumbing system because of a longer magma residence time in the crust (see below).

2. Data and Methods

To acquire new information about the stress state, the deformation pattern in the crust beneath and around Mount Etna, and the lithospheric setting of Eastern Sicily, we have referred both to original and large-scale geological/geophysical data sets available from the literature.

Original data consist of a 3-D strain model constructed for the whole of eastern Sicily, where the volcano is situated. The three-dimensional distribution of the strain in the crust below Mount Etna has been derived by calculating the horizontal strain rate from the seismic moment tensors by selecting earthquakes in the spatial domain of the whole of eastern Sicily and within a seismogenic depth of 50 km. After creating a sparse grid of cylinders with a radius of 25 km (one coinciding with the volcano area), the full strain rate tensors from the moment tensors for all these volumes were calculated using the Kostrov (1974) approach, where each earthquake represents an increment of strain. The increment is calculated as an equivalent homogeneous strain of the volume containing the seismogenic fault. The three-dimensional distributed strain tensor has been calculated by taking into account about 200 earthquakes recorded in the last 40 years for which a full moment tensor is available and by adopting a Gaussian kernel applied to each earthquake. The formulation is

$$\dot{\varepsilon}_{ij}(x, y, z) = \frac{d}{2\mu T\sqrt{\sigma_h\sigma_v}}\sum_k M_{ij}^{(k)} e^{-\frac{1}{2}\left[\frac{(x-x_k)^2+(y-y_k)^2}{\sigma_h^2}+\frac{(z-z_k)^2}{\sigma_v^2}\right]}$$

where $M_{ij}^{(k)}$ is the ij component of the moment tensor of the kth earthquake, μ is the rigidity modulus, T is the considered time span, and d, σ_h, and σ_v are the free parameters. The three free parameters have been chosen to optimize the fit with the strain rate calculated using the Kostrov approach in the grid of cylinders. The near-surface strain rate was calculated by adopting Shen et al. (1996) algorithm by using the GPS velocity field estimated by Palano et al. (2012) and Devoti et al. (2017) for Eastern Sicily.

Information on how deformation is currently dissipated in the crust comes from the analysis of the location of seismic events recorded in the area and of their focal solutions. Considered events are those recorded in the period 1981–2014 and were selected by taking account of minimum pre-requisites of quality (i.e., at least seven arrival-time observations) and, for the Mount Etna zone, a minimum magnitude of 2.5, to better highlight the main tectonic structures beneath the volcano. The relocation of earthquakes (see Scarfi et al., 2018), was performed using a 3-D velocity model and the tomoDDPS algorithm (Zhang et al., 2009). Fault plane solutions of earthquakes were selected from available studies (De Guidi et al., 2015) and catalogs (i.e., "Sicily and southern Calabria focal mechanisms catalog," http://sismoweb.ct.ingv.it/focal; RCMT, http://www.bo.ingv.it/RCMT; and TDMT, http://cnt.rm.ingv.it/tdmt). They have a magnitude ranging from 1 to 4.9 and a depth greater than 6 km (since at the shallower levels, the stress field is governed by the combination of the strong pressurization of the magmatic system and the dynamics of the shallower structures of the volcano). Available seismic tomography, derived from a high-resolution seismic velocity modeling (Scarfi et al., 2018), was also analyzed to image the lithospheric setting beneath eastern Sicily. Finally, we used geodetic baselines to acquire information on the ground deformation pattern affecting the volcanic edifice. We refer to distance measurements between benchmarks located on the western flank of the volcano; this sector

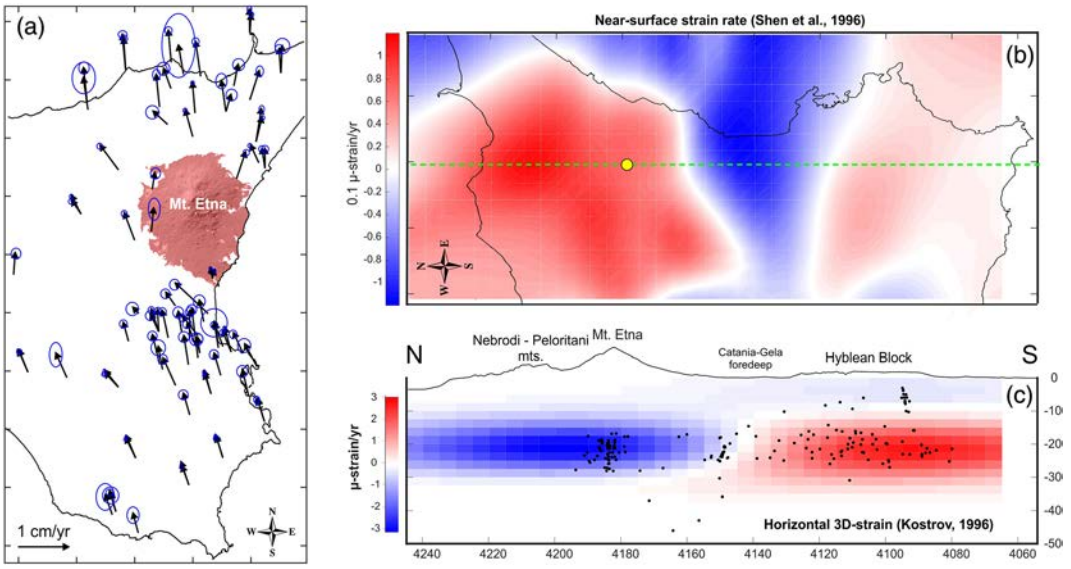

Figure 4. Near-surface and crustal strain rate field at Mount Etna. (a) GPS velocity field (black arrows) across eastern Sicily from Palano et al. (2012) and Devoti et al. (2017) in the Europe fixed reference frame and associated 95% confidence ellipses. (b) Dilatation strain rate at surface calculated by adopting a dedicated algorithm (see section 2) based on GPS displacement rates. (c) Section in depth of the horizontal dilatation rate calculated from seismic moment tensors (earthquakes in black dots). The profile refers to the green dashed line in (b). The yellow circle represents the summit of Mount Etna.

is preferable for evaluating inflation/deflation magmatic phases as it is not affected by faulting, eruptive fracturing, and flank instability (Bonaccorso, 2001). Here, distances have been routinely monitored since 1977 through different techniques, such as EDM (Electro-optical Distance Measurements), GPS, leveling and continuous tilt (Bonaccorso et al., 2015). However, in the analyzed time-window, a baseline measured using a unique technique is not available, and therefore we chose five baselines (according to the respective availability in time), measured using the GPS discrete or continuous techniques. To obtain a single continuous time series, the five baselines were harmonized and superimposed. The dilating rate was estimated by dividing the distance variation (about 0.3 m, excluding the permanent abrupt steps due to the dike-forming intrusions) by the medium value of the five baselines (about 7,500 m) and by the duration of the analyzed time-interval (four decades). Results are reported in section 4.

3. The Stress-Strain in the Crust Beneath the Volcano

In eastern Sicily, the current deformation field is well documented by more than 30 years of instrumental observations. Available GPS velocities (Figure 4a; Devoti et al., 2017; Palano et al., 2012) show the geodetic velocity of the Hyblean block (the lower plate) and the Nebrodi-Peloritani region (a stretched upper plate). The calculated near-surface strain field shows a positive horizontal strain in most of the Etnean area and to the north, whereas contraction (> -1 μ-strain/yr) is recoded immediately south of the volcano along the Catania-Gela foredeep (Figure 4b). Although the GPS differential velocities apparently indicate a slight extension between upper and lower plates, the crust beneath Mount Etna is instead affected by shortening, as indicated by the horizontal dilatation component of the calculated 3-D strain field, which is negative (about -3 μ-strain/yr, Figure 4c) in the crust below Mount Etna.

The location of earthquakes recorded in the area (Figure 5a) in the last 35 years (see adopted parameters in section 2), their focal mechanisms (Figure 5b) and available crustal and tomographic sections (Lavecchia et al., 2007; Scarfi et al., 2018), provide precise information of how and where tectonic shortening is being accommodated in the crust.

All the data suggest that deformation is expressed by a large, SE verging thrust ramp (see also De Guidi et al., 2015; Lavecchia et al., 2007) forming overall a deep-seated (up to 35 km in depth) shear zone

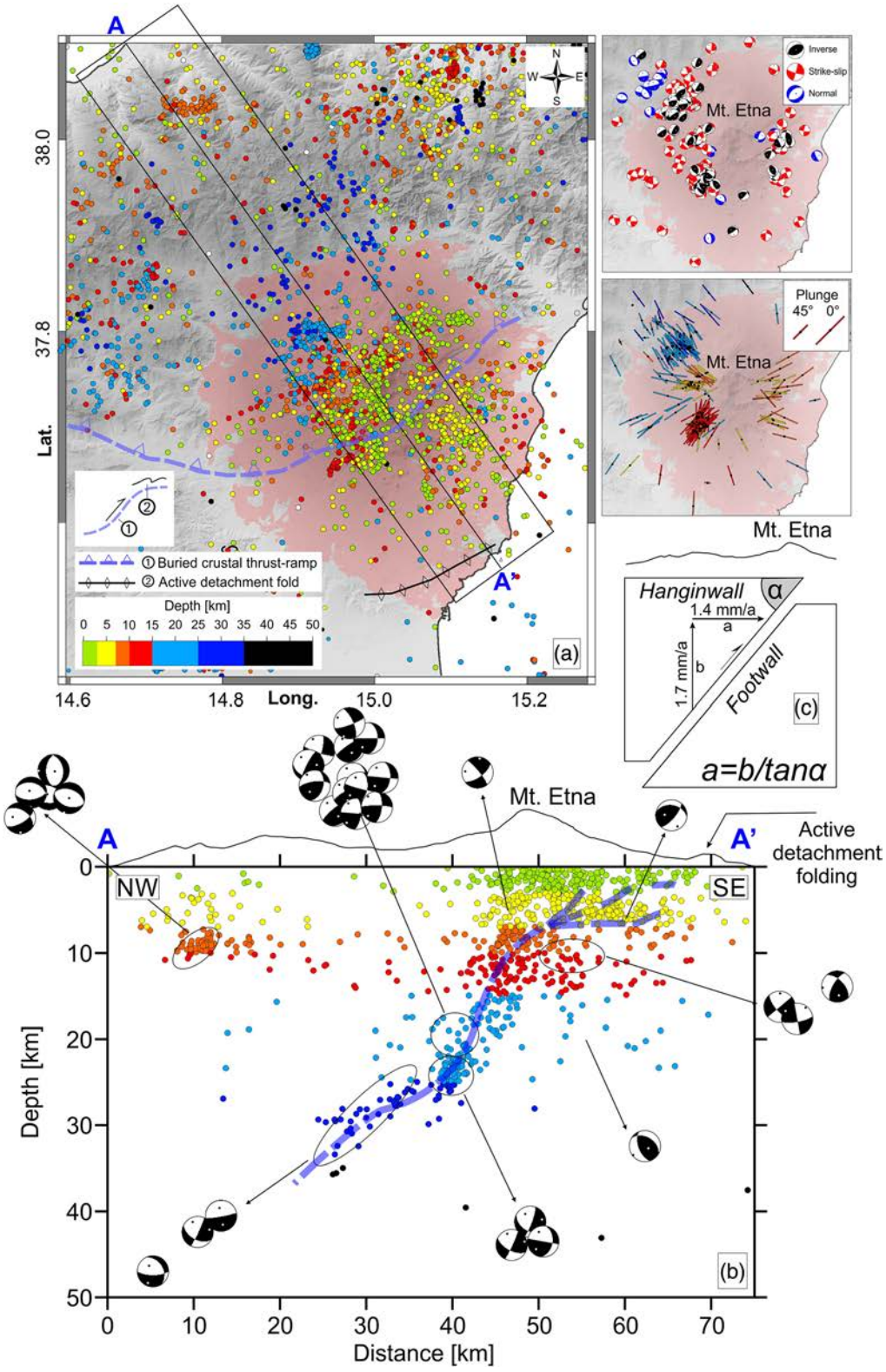

Figure 5. Seismicity distribution in the Etnean area. (a) Left, map of selected earthquakes recorded during the period 1981–2014; right, focal mechanisms and their *P* axes trending and plunging (colors are according to their type and depth, respectively (see palette in Figure 5a). (b) Cross-section view with earthquakes illuminating the thrust ramp. Focal solutions are for the events with magnitude ≥3.5 (trace and width of the section are shown in Figure 5a). Background map is DTM extracted from SRTM (Shuttle Radar Topography Mission) 30 plus topography (http://topex.ucsd.edu/WWW_html/srtm30_plus.html. (c) Calculated shortening rate beneath Mount Etna using long-term uplift rate for the Etna's basement and thrust inclination.

directly beneath the volcano (Figure 5b). Plan view (Figure 5a) and 3-D location of the earthquakes (Figure 5b) underline the occurrence of a NW dipping, NE-SW trending tectonic structure propagating at depth in the NW sector of Mount Etna roughly across its central crater zone. Tectonic motion along this structure is constrained by a large number of earthquakes with compressive focal solutions (Figure 5a, top right panel and Figure 5b). The nucleation of a single thrust-ramp directly beneath the volcano may suggest that deformation has exploited a preexisting zone of crustal weakness, probably the highly fractured zone hosting the early Mount Etna feeding system. Deactivation (about 200 ka ago, Ristuccia et al., 2013) of the shallow, short-wavelength fold and thrust system deforming the Mount Etna basement (Figure 1c) provides clues to when propagation of the deep-seated crustal thrust ramp started (De Guidi et al., 2015; Lavecchia et al., 2007). Estimation of the long-term uplift rate for the Mount Etna Pleistocene basement (1.3 and 1.7 mm/yr for the southern and northern sectors of the volcano, respectively, see Di Stefano & Branca, 2002; Monaco et al., 2002; Ristuccia et al., 2013) allows calculating a long-term shortening rate of 1.4 mm/yr. (Figure 5c) over the N dipping, 50° inclined (Figure 5b) thrust contact. The depth distribution of earthquakes indicates that the thrust contact cuts the whole lower plate. However, although the deep-seated thrust is well depicted by the earthquake's epicenters, no ground expressions have been observed at the surface along its ideal updip projection. Following previous interpretations (e.g., De Guidi et al., 2015) and considering the earthquakes' distribution in the shallow crust beneath the southern portion of the volcano (Figure 5b), the major thrust is characterized by flat-ramp geometries. The tectonic contact appears to change its trajectory approaching the surface (~5 km depth, Figure 5b) where it becomes flat, probably following a rheological contrast in the crust occurring between the rigid Hyblean carbonates and the tectonically overlaying terrigenous nappes of the Sicilian fold and thrust belt (Torelli et al., 1998). Thrust propagation over a flat decollement allows the possible vertical offset of the major thrust ramp to be transferred laterally, producing detachment folding at the surface. These fold structures are currently growing west and north of Catania at a rate of about 10 mm/yr (see Bonforte et al., 2011; Lundgren et al., 2004). Although geophysical data have highlighted deep-seated compressional stress in the crust beneath Mount Etna (see also Cocina et al., 1997; Lanzafame et al., 1997; Patanè & Privitera, 2001), diverging GPS vectors measured on the lower plate (including the Hyblean and Adria blocks, see D'Agostino & Selvaggi, 2004; Mastrolembo Ventura et al., 2014; Palano et al., 2012; Ward, 1994; see brown arrows in Figure 1a) indicate that oblique extension could persist along the eastern flank of the volcano (Monaco et al., 2005, 1997) and in the Ionian offshore (Barreca, Corradino, et al., 2018; Gutscher et al., 2016) according to a resultant ESE-WNW oriented vector (see yellow arrows in Figure 1a). In this context, contraction and extension appear to work simultaneously even if the very low rate of migration of the Calabrian trench to the east (~2 mm/yr, see D'Agostino et al., 2011) and the near-cessation of the Ionian slab rollback (Faccenna et al., 2001; Goes et al., 2004) implies a residual transtension at the slab edge in the eastern sector of the volcano and therefore a prevailing deep-seated contraction underneath.

4. Effects of Contraction and Crustal Thickening in the Mount Etna Volcanic System

According to the reconstructed stress state in the crust beneath Mount Etna (see section 3), we explore the possibility that most of the previously described variations (i.e., geochemical changes, increase in flank and in explosive eruptions, see section 2) could have been caused or conditioned by the deep-seated contraction. About 330 kyr ago, the tectonic inversion from extension to contraction probably caused the end of the foreland crustal stretching and related tholeiitic volcanism (Branca, Coltelli, Groppelli, & Lentini, 2011, and reference therein). Crustal shortening (i.e., during the 100-ka hiatus) and subsequent rupture and propagation of the large thrust ramp (i.e., since about 200 ka, see section 3 and Figure 5b), thickened the crust up to 35 km beneath Mount Etna (see Scarfi et al., 2018), producing lithostatic overload in the area. Following the lithostatic pressure calculation ($L_p = \rho g h$, where ρ is the density of the crust, g is the gravitational acceleration, and h is the height of rock column), a crustal thickening on the order of +10 km compared to the adjacent Hyblean sector would produce +250 MPa of overburden pressure, considering 2,700 Kg/m^3 as the average density for continental crust rocks. This additional lithostatic load probably inhibited mantle decompression in the source region below Mount Etna, favoring a lower degree of mantle melting and therefore the generation of alkali rather than tholeiitic magma (see Frost & Frost, 2019; Tanguy et al., 1997; Yoder & Tilley, 1962, and references therein).

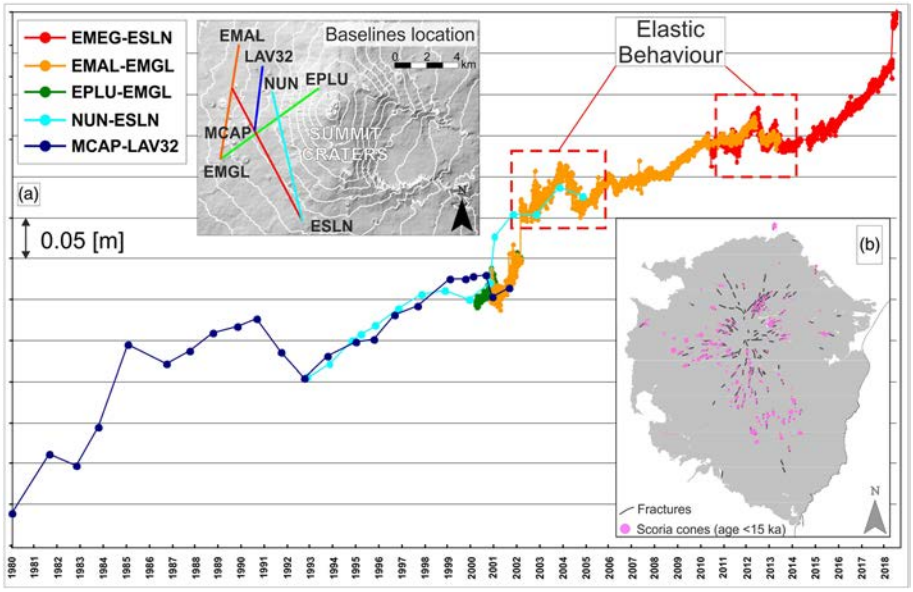

Figure 6. Continuous inflation at Mount Etna. (a) Time-series (1980–2018) of the length variations between some benchmarks located in the western part of Mount Etna. The hysteresis pattern is interpreted as related to continuous inflation due to magma storage within the volcano and attests to magma having difficulty in reaching the surface. Radial fracturing affecting the whole volcano (b) is here considered as the expression of volcano doming resulting from progressive magma accumulation within it.

As reported in section 1, the switch from subalkaline to alkaline magmas occurred about 200 ka, right after the 100-kyr hiatus in the volcanic activity (Branca, Coltelli, & Groppelli, 2011; De Beni et al., 2011). We also suggest that since 200 ka, the increased lithostatic load along with structural barrier nucleation (see also Gudmundsson, 2003, 2006), probably had an important role in the gradual stabilization and centralization of the plumbing system of Etna (see also Branca, Coltelli, & Groppelli, 2011) with magma ascending along few localized paths following inherited or newly formed crustal fault and fracture systems (see also Tibaldi et al., 2010). Furthermore, the formation of a structured plumbing system would have lengthened the period of magma storage in the crust, favoring fractional crystallization processes. The most striking effect of these processes manifested during the Ellittico volcano stage (60–15 ka, see Figure 2), when magma composition evolved from alkali-basalt to trachyte due to the cooling, crystallization, and exsolution of volatiles, whose accumulation finally triggered Plinian eruptions that concluded the Ellittico activity (around 15 ka; Coltelli et al., 2000).

A high-velocity V_P volume, interpreted as a main solidified intrusive body, has been found/imaged within Mount Etna through tomographic techniques and petrographic studies (Corsaro et al., 2014; Patanè et al., 2006). Indeed, huge intrusive emplacements of plutonic rocks are to be expected along volcanoes involved in contraction (Cas & Wright, 1987).

Since 1980, routinely monitored distance measurements between benchmarks located in the western part of the Mount Etna volcanic edifice (away from the unstable eastern flank) have revealed continuous inflation (Figure 6a).

Except for the abrupt steps observed during dike-forming intrusions, the volcanic edifice has been dilating at a roughly constant linear rate of 0.9 μ-strain/yr. The observed increasing dilatation pattern indicates that a substantial part of the rising magma has remained trapped inside the volcano rather than erupting, suggesting an inefficient magma transfer from the plumbing system to the surface (Tibaldi, 2015). The radially-oriented pattern of fractures (Figure 6b) pervasively affecting Mount Etna (as few other volcanoes in the world) is here seen as the result of doming by magma accumulation and cooling within the volcano (e.g., the high-velocity V_P volume, see above). In this context, dikes can also contribute to the permanent inflation, owing to difficulty in reaching the surface as they are forced to propagate through a crust under contraction (Gudmundsson, 2003, 2006). Short-period, bell-shaped inflation/deflation pattern (e.g., across the

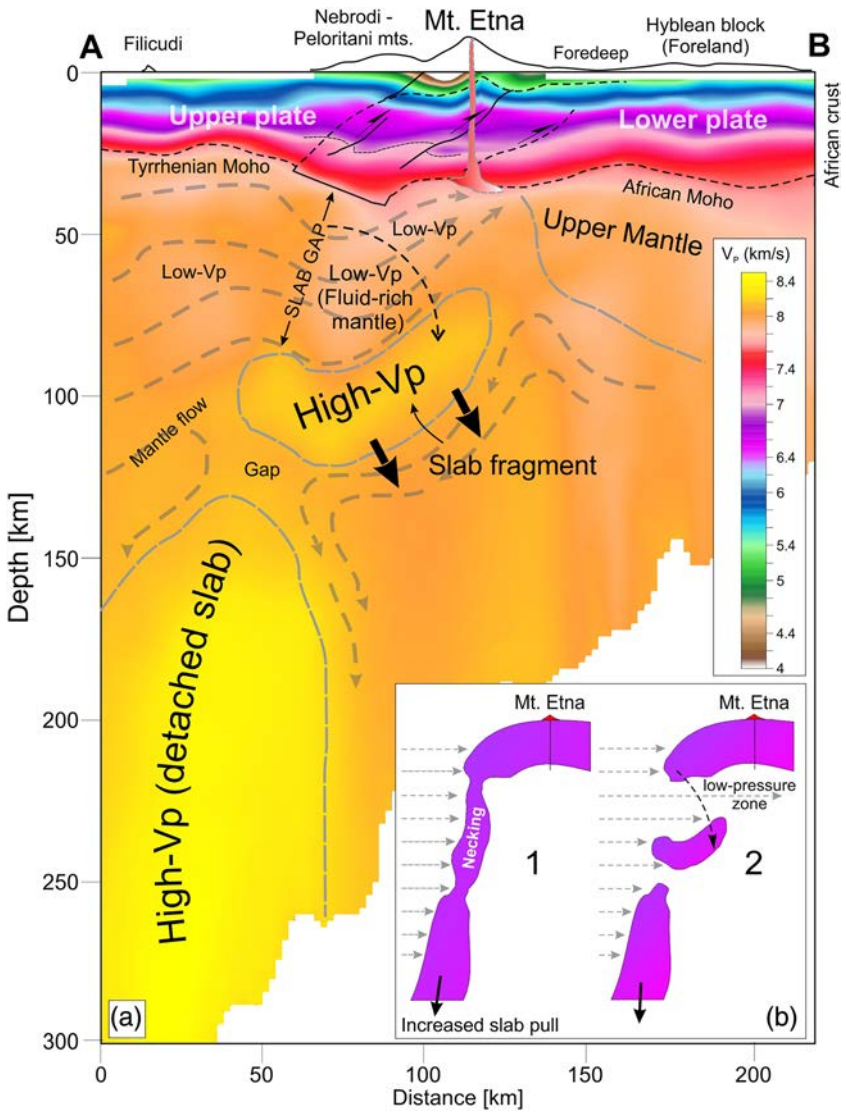

Figure 7. (a) Tectonic interpretation over a vertical section through available *Vp* model (data are from Scarfi et al., 2018) showing the fragmented slab and associated gap north of Mount Etna (trace location in Figure 9a). The low-*Vp* zone is interpreted as a less dense material (a lighter suprasubduction mantle wedge) penetrating in the Etnean region. (b) Cartoon model based on the tomography showing slab necking (1) and gap opening mode (2).

2004 and 2013 eruptions, red dashed boxes in Figure 6a) show that occasionally inflation is completely rebalanced after eruptive events, suggesting an elastic behavior of the involved medium. This behavior allows us to disprove that hysteresis could be related to a nonelastic state of Etnean rocks. The age of scoria cones associated with most of the radially oriented volcanic fractures provides insights to extend the continuous inflation process back in time to the last 15 ka.

Considering the contraction of the crust below the volcano, the increased number of flank eruptions in the last few thousands of years could be seen as an effect of tectonic overload and shortening, which favored more diffuse and efficient magma transport pathways (see also Tibaldi et al., 2010), resulting in the emplacement of more than 250 peripheral scoria cones in the last 15 ka (Figure 6b).

5. Slab Detachment and Geodynamic Implications on Volcanism

Deepening of thrusting in the Mount Etna area (originally developed in a shallower tectonic setting, the inner portion of the Catania-Gela foredeep, Figure 1b) must be related to a significant geodynamic

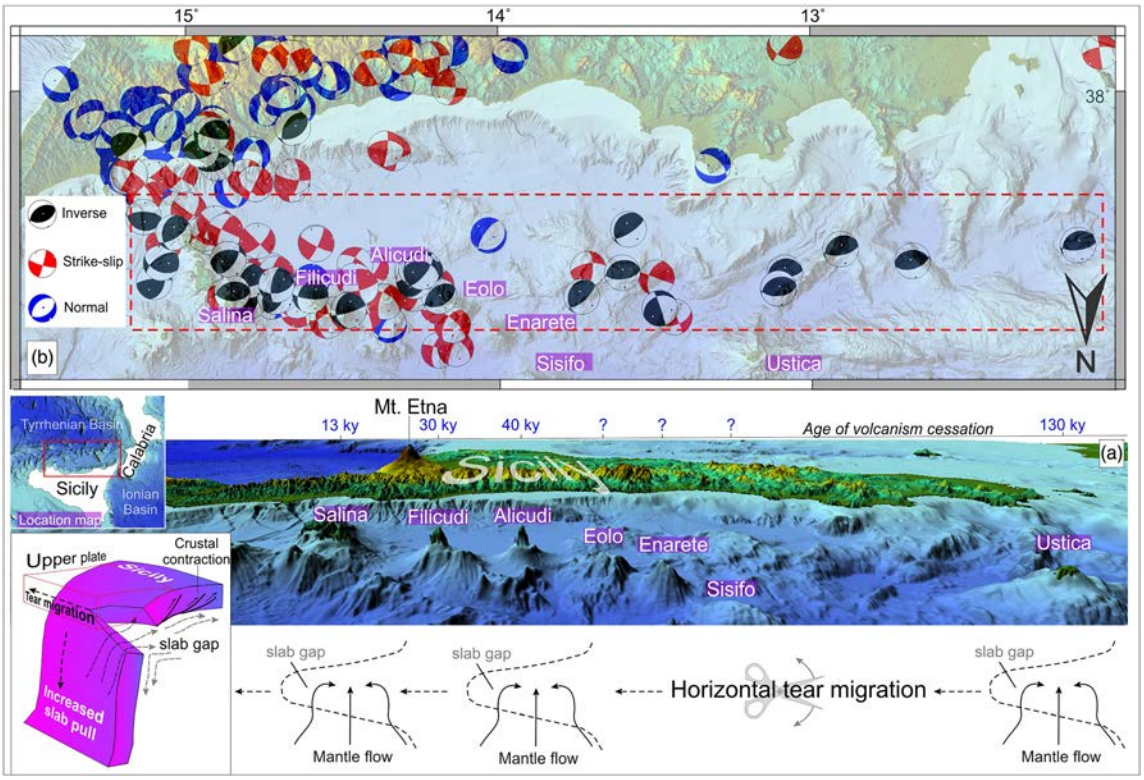

Figure 8. (a) Perspective view from the north of the southern Tyrrhenian margin (see the location map in the top left) showing extinct volcanoes in the area. Age of volcanism cessation, older to the west and younger to the east, suggests the originally continuous Ionian slab as detached in a scissor-type mode (see Faccenna et al., 2005, 2007, and cartoon in the bottom left; Wortel & Spakman, 2000), tearing diachronically toward the east. (b) Progressive opening of a slab gap favored fore-arc mantle migration toward the south and the inception of deep-seated contraction in the overlying crust. Deep-seated crustal shortening in the area is demonstrated by the reverse kinematics of most of the available focal solutions (Pondrelli, 2000; Scarfi et al., 2013, 2016, depth range 10–38 km) whose distribution depicts a roughly E-W trending contractional belt (red dashed rectangle). Strike-slip deformation becomes predominant toward the east, depicting the modern slab edge tearing (see Barreca et al., 2014; Cultrera et al., 2017).

reorganization in the area. A tectonic interpretation performed over an available tomographic section (Scarfi et al., 2018) allowed us to image the architecture of the lithospheric system below the analyzed area. The tomographic section (Figure 7) clearly suggests the occurrence of two high-velocity bodies ($Vp > 8$ km/s) that, following previous authors (Calò et al., 2012; Neri et al., 2009; Scarfi et al., 2018), we interpret as fragments of a detached slab, accounting thereby for a trench-parallel slab breakoff with the consequent opening of a large horizontal slab window just north of Mount Etna (Figure 7a). In particular, the position of the thinned and uppermost fragment provides insights into the detaching process, which has probably occurred by necking of the oceanic lithosphere in response to the increased downward-pulling forces. According to the notion that slab retreat must either be compensated or pushed by the supra-adjacent mantle (Doglioni et al., 1999; Faccenna et al., 2011), the opening of a slab gateway into the subducting Ionian oceanic lithosphere could have induced a lighter (fluid-enriched) suprasubduction mantle wedge (originally feeding volcanism at Alicudi and Filicudi, currently inactive) to flow through the slab gap up to wedge below the Mount Etna region.

This process was probably favored by lithospheric delamination (and possibly accompanied by thermal erosion) that occurred below the Nebrodi-Peloritani Mountains (Figure 7a), according to which the subcontinental upper-mantle decoupled from the crust and was progressively replaced by the southward moving fore-arc mantle wedge. Furthermore, about 50° horizontal-axis clockwise rotation (from its original position) of the uppermost slab fragment (Figure 7b-1) suggests that, after being detached, it was pushed and rotated by the advancing fore-arc mantle (Figure 7b-2). A low-velocity zone recently found through tomographic images (Scarfi et al., 2018), together with a local gravity anomaly minimum and relative maxima of heat flow just north of Mount Etna (see Barreca, Branca, & Monaco, 2018, and Figure 9c) support penetration of less dense material in the Etnean region.

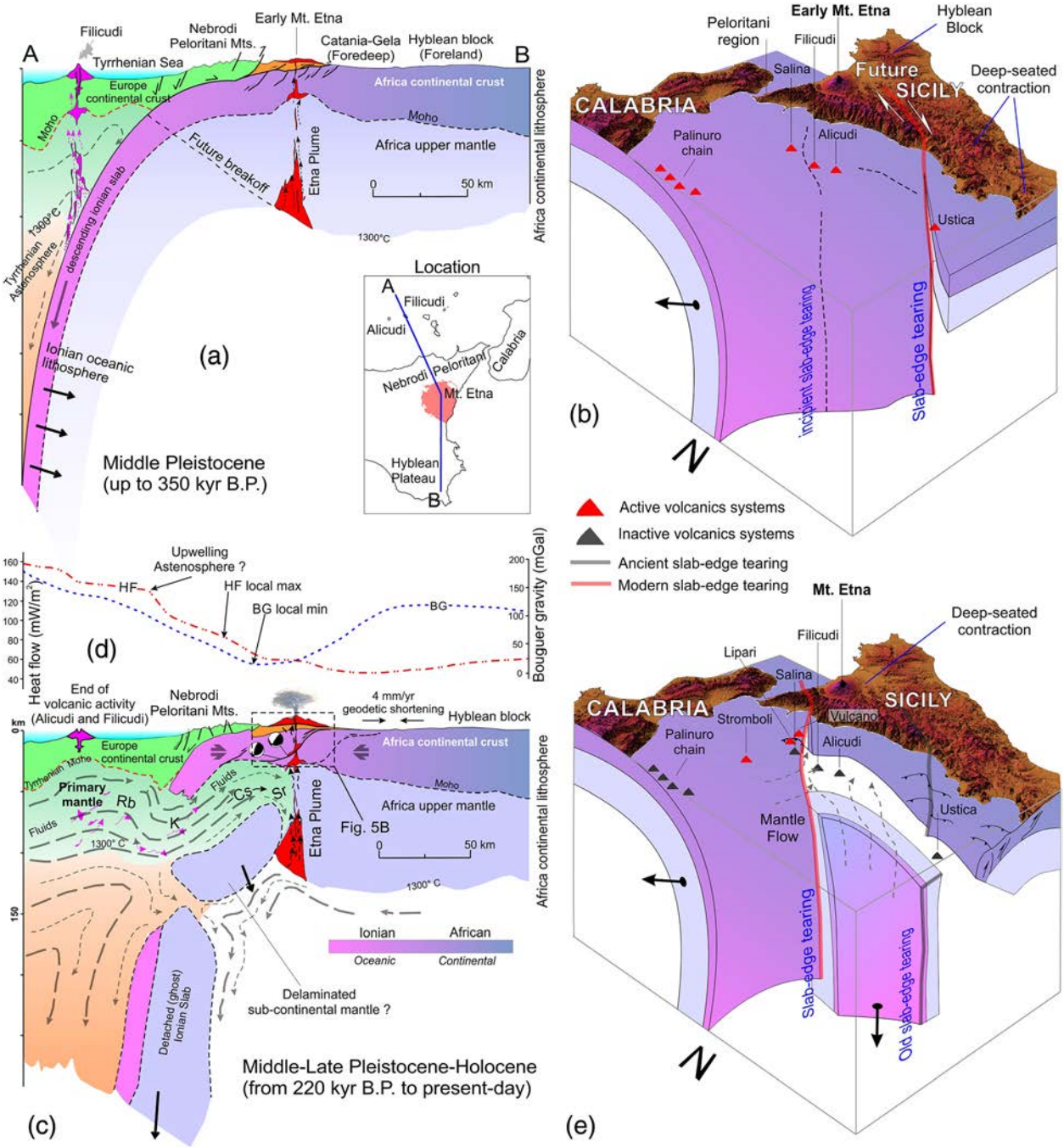

Figure 9. Geodynamic evolution of the lithospheric system beneath the Mount Etna volcano and western Eolian arc regions. (a) Scenario at Middle Pleistocene (up to 350 ka BP) when volcanism was still active in the western part of the Eolian arc (i.e., at Alicudi and Filicudi) implying that the Ionian slab was still continuous beneath the two volcanic islands. (b) 3-D model with a perspective view from NW. (c) The end of volcanic activity at Alicudi and Filicudi islands is the expression of subduction cessation in the area as a consequence of trench-parallel breakoff of the Ionian slab, a process clearly depicted by tomographic images (Calò et al., 2012; Neri et al., 2009; Scarfì et al., 2018, see Figure 7). The opening of a gap into the Ionian slab originally separating the two lithosphere/asthenosphere systems (i.e., Tyrrhenian to the north and the Hyblean to the south) allowed the less dense, fluid-enriched and warmer suprasubduction mantle wedge to be mobilized toward the south until its penetration in the Etnean region. This process is also supported by heat flow (Della Vedova et al., 2001) and gravity (Morelli, 1997) trends in the area (d) and is here considered as responsible for magma source contamination (island arc vs. plume, see Schiano et al., 2001) and deep contraction in the Mount Etna area. (e) 3-D block models (perspective view from the NW) displaying the propagation of trench-parallel slab break-off in a scissor-type mode (see also Wortel & Spakman, 2000, and Figure 8) allowing occasional mantle mobilization through the slab gap and deep-seated contraction in the overlying crust with progressive volcanism cessation along the southern margin of the Tyrrhenian Basin. Depleted mantle replaced by primary mantle below Alicudi and Filicudi volcanic islands represents the evidence for this kind of process. The figure has been partly redrawn from Barreca, Branca, & Monaco, 2018) and is mostly based on available tomographic model (Figure 7, see also Scarfì et al., 2018).

Higher K/Na, Mg/Al, Rb/Sr, and lower Ba/Nb, Ba/Rb ratios recorded in the last volcanic activity of the western Eolian Arc are considered to reflect magma derivation from a mantle source that is different from the original MORB-like source (Santo et al., 2004). Variations in the ratios suggest that the (depleted) mantle wedge initially feeding the western Eolian Arc volcanic system might have been pushed and replaced by primary mantle coming from the north in line with slab-hinge retreat toward the south. The transition of Mount Etna lavas from a mantle-plume (Peccerillo, 2017) to an island arc magmatic source, based on petrologic data (Corsaro & Pompilio, 2004; Peccerillo, 2017; Schiano et al., 2001), confirms that mantle has flowed from the nearby Eolian sector, also leading Mount Etna to reach eruption rates near to that of oceanic arc volcanic systems in the last 60 ka (Barreca, Branca, & Monaco, 2018). Following the southward mantle migration, the intraplate (Africa/Ionian) crustal shortening below Mount Etna is here interpreted as the result of a far-field geodynamic process triggered by the trench-parallel breakoff of the Ionian slab (see above).

Trench-parallel slab detachment and related mantle flow have probably already occurred along the southern Tyrrhenian margin (Figure 1a), a process that seems to have left behind a cemetery of volcanoes with the cessation of activity associated with both slab edge tearing and subduction-related volcanic systems. The time-progressive cessation of volcanism from west to east (130 ka at Ustica, see Bousquet & Lanzafame, 1995, 30–40 ka at Alicudi and Filicudi, 13 ka at Salina, see Barreca et al., 2014; Figure 8a), suggests an opening of the horizontal slab window from west to east in a scissor-type mode (Faccenna et al., 2005, 2007; Wortel & Spakman, 2000). This process has favored a progressive southward mobilization of the fore-arc mantle, producing deep-seated shortening in the overlying crust. Crustal shortening is currently testified by the occurrence, all along the southern Tyrrhenian margin, of several earthquakes with reverse focal mechanisms roughly delineating an E-W contractional belt (Figure 8b).

Moreover, the near-cessation of the Calabrian rollback and current stalling of the slab subduction (Faccenna et al., 2001; Goes et al., 2004) also eastward (i.e., east of the modern slab edge tear fault, Figure 1a) will imply a reduced tectonic activity by lithospheric tearing at the slab edge, since edge tears propagate only if a slab rolls back (Govers & Wortel, 2005). Accordingly, the deep tear in the lithosphere, invoked to explain Mount Etna's origin and considered the preferential dilatational pathway for magma ascent in the area (Doglioni et al., 2001; Gvirtzman & Nur, 1999; Hirn et al., 1997), may be involved later in the incipient deeper contraction that is a prelude to its complete positive tectonic inversion. A geodetic shortening rate of 3 mm/yr, documented by GPS velocities between Lipari and Vulcano islands (Barreca et al., 2014), namely along the northern tip of the modern slab edge tear, confirms this tendency. Cessation of volcanism occurred 300 ka (Savelli, 2002) at the northern slab edge tear of the Calabrian/Ionian subduction zone (i.e., in the Vulture volcano, De Astis et al., 2006, D'Orazio et al., 2007, and along the Palinuro Volcanic Chain, Cocchi et al., 2017, De Ritis et al., 2019, Figure 9), could represent an analog of the scenario expected for Mount Etna, the latter being located atop the southern slab edge tear fault (Figure 1a).

6. Discussion and Conclusions

We have proposed that Mount Etna volcanism is now controlled by the convergent tectonic forces that have manifested in the area with crustal shortening affecting the lower plate (Africa/Ionian) of the collisional system. This geodynamic change probably occurred about 330 ka, and it is supported by the deepening of thrusting in the area. Accordingly, since this time, the evolution of Etnean volcanism is no longer related to the extensional foreland dynamics (with production of tholeiitic magmas similar to the Hyblean one; see Branca, Coltelli, & Groppelli, 2011, and references therein) but rather have become strictly related to Africa-Europe collision (deep thrusting) and Ionian subduction, with the latter strongly influenced by lateral and along-strike slab detachment (see also Barreca et al., 2016; Doglioni et al., 2001; Gvirtzman & Nur, 1999; Hirn et al., 1997). The arrival of the buoyant and thicker Africa continental lithosphere in the western part of the Ionian subduction zone (i.e., west of the modern slab edge tearing faulting, Figure 1a) clogged the subduction north of Mount Etna (Figure 9a). This induced slab-steepening, rollback deceleration, and then stalling of the slab until its complete detaching by increased downward-pulling forces.

Gateway opening into the subducting slab facilitated the southward mobilization of a lightened fore-arc mantle, giving rise to magmatic source mixing in the Etnean area (see also Schiano et al., 2001) together with the inception of contractional tectonics in the crust below the volcano (Figure 9b).

The present geodynamic setting, dominated by deep-seated contraction, represents an unfavorable scenario for the continuation of volcanism (Glazner, 1991; Hamilton, 1995) as also suggested by the 100-kyr hiatus. Stable long-term uplift rates, related to regional geodynamics (see Di Stefano & Branca, 2002; Monaco et al., 2002; Ristuccia et al., 2013), allow us to exclude the possibility that during this time span, plutonic emplacement has occurred at depth, since strong local uplift is expected in response to such a process. However, field evidence and physically-scaled experiments suggest that volcanism can also persist in contractional settings (Tibaldi, 2008). According to the age inferred for the onset of crustal shortening, Mount Etna volcanism has resisted contraction for about 330 ka. During this period, magma possibly used newly formed, roughly N-S trending tensile fractures parallel to the direction of maximum stress axis (Tibaldi, 2008, Nakamura & Uyeda, 1980, see also *P* axes trending in Figure 5) or preexisting transtensional tectonic structures (whose activity prevailed before 330 ka, Monaco et al., 1997) to reach the surface, whereas source contamination by subduction-related components (Schiano et al., 2001) along with a gradual stabilization of the plumbing system (Branca, Coltelli, & Groppelli, 2011) have guaranteed an increase in the eruption rates (Barreca, Branca, & Monaco, 2018; Branca & Ferrara, 2013) favoring the construction of huge stratovolcanoes, typical of island-arc settings.

In a similar geo-tectonic context, shortening at a rate of 1.4 mm/yr (see section 3), magma stalling in the crust because of structural (i.e., reverse faults) and stress barriers (see Gudmundsson, 2011; Moran et al., 2011) and possible conduit bottlenecks under a deep-seated and nearly horizontal maximum stress axis (Figure 5a, bottom right panel) should imply longer magma storage times, more gas accumulation, and horizontal magma migration with a possible consequent future increase in highly energetic explosive activity and the opening of eruptive fissures along the flanks. According to the ongoing geodynamics and the calculated rate of tectonic shortening, all the abovementioned anomalous signals (increase in flank and in explosive eruptions in the last 15 ka, continuous inflation with the resulting pervasive, radially arranged fracturing deforming the whole volcano; see Figure 6b) would seem to suggest that the dynamics of Mount Etna's volcanic system is experiencing a significant change, in line with its crustal root undergoing deep-seated contraction. As already occurred in almost all volcanoes lying atop a detached slab in the Southern Tyrrhenian margin (see section 5 and Figure 9), and considering that slab opening has now reached the sector north of the volcano (Figure 7), a decline of volcanism cannot be ruled out also in eastern Sicily. Just how long volcanism will resist the contraction, however, cannot be determined. In the current stage, the dilatation dynamics affecting the eastern flank of the volcano (mostly tectonic and gravity-driven, Barreca, Corradino, et al., 2018; Bonforte et al., 2011; Lundgren et al., 2004; Puglisi & Bonforte, 2004; Rust et al., 2005; Walter et al., 2005) has ensured the quasi-continuous depressurization of the volcanic system (Branca et al., 2003) favoring degassing, magma intrusion along the flanks, and the fast ascent along the central feeder system up to now.

To conclude, this paper suggests that slab narrowing by progressive lateral detaching and related suprasubduction mantle mobilization may have a strong influence in controlling the evolution of magmatic systems facing subduction zones.

Acknowledgments

J. Malavieille, two anonymous reviewers, and the Editors are kindly acknowledged for their constructive comments and suggestions. We also thank Alessandro Bonaccorso and Alessandro Bonforte for making available two of the baselines shown here available (MCAP-LAV32 and NUN-ESLN). The authors acknowledge the use of MOVE Software Suite granted by Petroleum Experts Limited (www.petex.com). The work benefits from grants from the University of Catania in the frame of the project "Multidisciplinary analysis of the deformation in the around of active tectonic structures (supervisor G. Barreca)."

Data Availability Statements

Seismic data sets for this research are included in Scarfi et al. (2018). Analyses of major and trace elements in bulk rocks of Mount Etna, which are plotted in Figure 3, are a collection from different laboratories summarized in Corsaro and Pompilio (2004). GPS data for the near-surface strain rate come from Palano et al. (2012) and Devoti et al. (2017). The geodetic baseline has been obtained by merging previous measurements which are included in Bonaccorso et al. (2015).

References

Armienti, P., Innocenti, F., Petrini, R., Pompilio, M., & Villari, L. (1989). Petrology and Sr-Nd isotope geochemistry of recent lavas from Mt. Etna: bearing on the volcano feeding system. *Journal of Volcanology and Geothermal Research*, *39*(4), 315–327. https://doi.org/10.1016/0377-0273(89)90095-4

Armienti, P., Perinelli, C., & Putirka, K. D. (2013). A new model to estimate deep-level magma ascent rates, with applications to Mt. Etna (Sicily, Italy). *Journal of Petrology*, *54*(4), 795–813. https://doi.org/10.1093/petrology/egs085

Armienti, P., Tonarini, S., D'Orazio, M., & Innocenti, F. (2004). Genesis and evolution of Mt. Etna alkaline lavas: Petrological and Sr–Nd–B isotope constraints. *Periodico Di Mineralogia*, *73*, 29–52.

Barberi, F., Civetta, L., Gasparini, P., Innocenti, F., Scandone, R., & Villari, L. (1974). Paleomagnetic and volcanological evidence from Sicily. *Earth and Planetary Science Letters*, *22*(2), 123–132. https://doi.org/10.1016/0012-821X(74)90072-7

Barreca, G., Branca, S., & Monaco, C. (2018). Three-dimensional modeling of Mount Etna volcano: volume assessment, trend of eruption rates and geodynamic significance. *Tectonics*, *37*, 842–857. https://doi.org/10.1002/2017TC004851

Barreca, G., Bruno, V., Cultrera, F., Mattia, M., Monaco, C., & Scarfì, L. (2014). New insights in the geodynamics of the Lipari–Vulcano area (Aeolian archipelago, southern Italy) from geological, geodetic and seismological data. *Journal of Geodynamics*, *82*(2014), 150–167. https://doi.org/10.1016/j.jog.2014.07.003

Barreca, G., Corradino, M., Pepe, F., & Monaco, C. (2018). Active tectonics along the south east offshore margin of Mt. Etna: New insights from high-resolution seismic profiles. *Geosciences*, *8*(2), 62. https://doi.org/10.3390/geosciences8020062

Barreca, G., Scarfì, L., Cannavò, F., Koulakov, I., & Monaco, C. (2016). New structural and seismological evidence and interpretation of a lithospheric-scale shear zone at the southern edge of the Ionian subduction system (central eastern Sicily, Italy). *Tectonics*, *35*, 1489–1505. https://doi.org/10.1002/2015TC004057

Barreca, G., Scarfì, L., Gross, F., Monaco, C., & De Guidi, G. (2019). Fault pattern and seismotectonic potential at the south-western edge of the Ionian subduction system (southern Italy): New field and geophysical constraints. *Tectonophysics*, *761*, 31–45. https://doi.org/10.1016/j.tecto.2019.04.020

Bonaccorso, A. (2001). Mt. Etna volcano: modelling of ground deformation patterns of recent eruptions and considerations on the associated precursors. *Journal of Volcanology and Geothermal Research*, *109*(1–3), 99–108. https://doi.org/10.1016/S0377-0273(00)00306-1

Bonaccorso, A., Bonforte, A., & Gambino, S. (2015). 25 years' continuous borehole tilt and vertical displacement data at Mt. Etna: Insights on long-term volcanic dynamics. *Geophysical Research Letters*, *42*, 10,222–10,229. https://doi.org/10.1002/2015GL066517

Bonforte, A., Guglielmino, F., Coltelli, M., Ferretti, A., & Puglisi, G. (2011). Structural assessment of Mount Etna volcano from permanent scatterers analysis. *Geochemistry, Geophysics, Geosystems*, *12*, Q02002. https://doi.org/10.1029/2010GC003213

Bousquet, J. C., & Lanzafame, G. (1995). Transition from Tyrrhenian basin extension to collisional tectonics: Evidence of N-S compression during the recent quaternary at Ustica (southern Tyrrhenian Sea, Italy). *C.R. Acad. Sci., Sér. 2, Sci. Terre Planètes*, *321*(9), 781-787.

Branca, S., Carbone, D., & Greco, F. (2003). Intrusive mechanism of the 2002 NE-Rift eruption at Mt. Etna (Italy) inferred through continuous microgravity data and volcanological evidences. *Geophysical Research Letters*, *30*(20), 2077. https://doi.org/10.1029/2003GL018250

Branca, S., Coltelli, M., De Beni, E., & Wijbrans, J. (2008). Geological evolution of Mount Etna volcano (Italy) from earliest products until the first central volcanism (between 500 and 100 ka ago) inferred from geochronological and stratigraphic data. *International Journal of Earth Sciences*, *97*(1), 135–152. https://doi.org/10.1007/s00531-006-0152-0

Branca, S., Coltelli, M., & Groppelli, G. (2011). Geological evolution of a complex basaltic stratovolcano: Mount Etna, Italy. *Italian Journal of Geosciences*, *130*(3), 306–317. https://doi.org/10.3301/IJG.2011.13

Branca, S., Coltelli, M., Groppelli, G., & Lentini, F. (2011). Geological map of Etna volcano, 1: 50,000 scale. *Italian Journal of Geosciences*, *130*(3), 265–291. https://doi.org/10.3301/IJG.2011.155

Branca, S., & Ferrara, V. (2013). The morphostructural setting of Mount Etna sedimentary basement (Italy): Implications for the geometry and volume of the volcano and its flank instability. *Tectonophysics*, *586*, 46–64. https://doi.org/10.1016/j.tecto.2012.11.011

Calò, M., Dorbath, C., Luzio, D., Rotolo, S. G., & D'Anna, G. (2012). Seismic velocity structures of southern Italy from tomographic imaging of the Ionian slab and petrological inferences. *Geophysical Journal International*, *191*(2), 751–764. https://doi.org/10.1111/j.1365-246X.2012.05647.x

Cas, R. A. F., & Wright, J. V. (1987). *Volcanic successions* (p. 528). London, UK: Allen and Unwin. https://doi.org/10.1007/978-94-009-3167-1

Chester, D. K., Duncan, A. M., Guest, J. E., & Kilburn, C. R. J. (1975). *Mount Etna: The anatomy of a volcano* (p. 404). London, UK: Chapman and Hall.

Cocchi, L., Passaro, S., Tontini, F. C., & Ventura, G. (2017). Volcanism in slab tear faults is larger than in island-arcs and back-arcs. *Nature Communications*, *8*(1), 1451. https://doi.org/10.1038/s41467-017-01626-w

Cocina, O., Neri, G., Privitera, E., & Spampinato, S. (1997). Stress tensor computations in the Mount Etna area (southern Italy) and tectonic implications. *Journal of Geodynamics*, *23*(2), 109–127. https://doi.org/10.1016/S0264-3707(96)00027-0

Coltelli, M., del Carlo, P., & Vezzoli, L. (2000). Stratigraphic constrains for explosive activity in the last 100 ka at Etna volcano, Italy. *International Journal of Earth Sciences*, *89*(3), 665–677. https://doi.org/10.1007/s005310000117

Condomines, M., Tanguy, J. C., Kieffer, G., & Allegre, J. C. (1982). Magmatic evolution of a volcano studied by 230Th-238U disequilibrium and trace elements systematics: The Etna case. *Geochimica et Cosmochimica Acta*, *46*(8), 1397–1416. https://doi.org/10.1016/0016-7037(82)90275-7

Condomines, M., Tanguy, J. C., & Michaud, V. (1995). Magma dynamics at Mt Etna - constraints from U-Th-Ra-Pb radioactive disequilibria and Sr isotopes in historical lavas. *Earth and Planetary Science Letters*, *132*(1–4), 25–41. https://doi.org/10.1016/0012-821X(95)00052-E

Corsaro, R. A., & Pompilio, M. (2004). Dynamics of magmas at Mount Etna. In A. Bonaccorso, S. Calvari, M. Coltelli, C. Del Negro, & S. Falsaperla (Eds.), *Mt. Etna: Volcano laboratory*, *Geophysical Monograph Series* (Vol. 143, pp. 91–110). Washington, DC: American Geophysical Union.

Corsaro, R. A., Rotolo, S. G., Cocina, O., & Gianvito, T. (2014). Cognate xenoliths in Mt. Etna lavas: witnesses of the high velocity body beneath the volcano. *Bulletin of Volcanology*, *76*(1), 772. https://doi.org/10.1007/s00445-013-0772-8

Cultrera, F., Barreca, G., Burrato, P., Ferranti, L., Monaco, C., Passaro, S., et al. (2016). Active faulting and continental slope instability in the Gulf of Patti (Tyrrhenian side of NE Sicily, Italy): A field, marine and seismological joint analysis. *Natural Hazards*, *86* (April 2017), S253–S272. https://doi.org/10.1007/s11069-016-2547-y

Cultrera, F., Barreca, G., Ferranti, L., Monaco, C., Pepe, F., Passaro, S., et al. (2017). Structural architecture and active deformation pattern in the northern sector of the Aeolian-Tindari-Letojanni fault system (SE Tyrrhenian Sea-NE Sicily) from integrated analysis of field, marine geophysical, seismological and geodetic data. *Italian Journal of Geosciences*, *136*(3), 399–417. https://doi.org/10.3301/IJG.2016.17

D'Agostino, N., Anastasio, E., Gersavi, A., Guerra, I., Nedimović, M. R., Seeber, L., & Steckler, M. S. (2011). Forearc extension and slow rollback of the Calabrian arc from GPS measurements. *Geophysical Research Letters*, *38*, L17304. https://doi.org/10.1029/2011GL048270

D'Agostino, N., & Selvaggi, G. (2004). Crustal motion along the Eurasia-Nubia plate boundary in the Calabrian arc and Sicily and active extension in the Messina Straits from GPS measurements. *Journal of Geophysical Research*, *109*, B11402. https://doi.org/10.1029/2004JB002998

De Astis, G., Kempton, P. D., Peccerillo, A., & Wu, T. W. (2006). Trace element and isotopic variations from Mt. Vulture to Campanian volcanoes: Constraints for slab detachment and mantle inflow beneath southern Italy. *Contributions to Mineralogy and Petrology*, *151*(3), 331–351. https://doi.org/10.1007/s00410-006-0062-y

De Beni, E., Branca, S., Coltelli, M., Groppelli, G., & Wijbrans, J. (2011). $^{39}Ar/^{40}Ar$ isotopic dating of Etna volcanic succession. *Italian Journal of Geosciences*, *130*(3), 292–305. https://doi.org/10.3301/IJG.2011.14

De Guidi, G., Barberi, G., Barreca, G., Bruno, V., Cultrera, F., Grassi, S., et al. (2015). Geological, seismological and geodetic evidence of active thrusting and folding south of Mt. Etna (eastern Sicily): Revaluation of "seismic efficiency" of the Sicilian basal thrust. *Journal of Geodynamics*, *90*, 32–41. https://doi.org/10.1016/j.jog.2015.06.001

De Ritis, R., Pepe, F., Orecchio, B., Casalbore, D., Bosman, A., Chiappini, M., et al. (2019). Magmatism along lateral slab edges: Insights from the diamante-Enotrio-Ovidio volcanic-intrusive complex (southern Tyrrhenian Sea). *Tectonics*, *38*, 2581–2605. https://doi.org/10.1029/2019TC005533

Del Carlo, P., Branca, S., & D'Oriano, C. (2017). New findings of late glacial Etna pumice fall deposits in NE Sicily and implications for distal tephra correlations in the Mediterranean area. *Bulletin of Volcanology*, *79*(7), 50. https://doi.org/10.1007/s00445-017-1135-7

Del Carlo, P., Vezzoli, L., & Coltelli, M. (2004). In A. Bonaccorso, S. Calvari, M. Coltelli, C. Del Negro, & S. Falsaperla (Eds.), *Last 100 ka Tephrostratigraphic record of Mount Etna*, *Geophysical Monograph Series* (Vol. 143, pp. 77–89). Washington, DC: Etna Volcano Laboratory AGU.

Della Vedova, B., Bellani, S., Pellis, G., & Squarci, P. (2001). Deep temperatures and surface heat flow distribution. In G. B. Vai & I. P. Martini (Eds.), *Anatomy of an Orogen: The Apennines and Adjacent Mediterranean Basins* (pp. 65–76). Dordrecht, Netherlands: Kluwer Academic. https://doi.org/10.1007/978-94-015-9829-3_7

Devoti, R., D'Agostino, N., Serpelloni, E., Pietrantonio, G., Riguzzi, F., Avallone, A., et al. (2017). A combined velocity field of the Mediterranean region. *Annals of Geophysics*, *60*(2). https://doi.org/10.4401/ag-7059

Di Renzo, V., Corsaro, R. A., Miraglia, L., Pompilio, M., & Civetta, L. (2019). Long and short-term magma differentiation at Mt. Etna as revealed by Sr-Nd isotopes and geochemical data. *Earth-Science Reviews*, *190*, 112–130.

Di Stefano, A., & Branca, S. (2002). Long-term uplift rate of the Etna volcano basement (southern Italy) from biochronological data of the Pleistocene sediments. *Terra Nova*, *14*(1), 61–68. https://doi.org/10.1046/j.1365-3121.2002.00389.x

Doglioni, C., Harabaglia, P., Merlini, S., Mongelli, F., Peccerillo, A., & Piromallo, C. (1999). Orogens and slabs vs their direction of subduction. *Earth Science Reviews*, *45*(3-4), 167–208. https://doi.org/10.1016/S0012-8252(98)00045-2

Doglioni, C., Innocenti, F., & Mariotti, S. (2001). Why Mt. Etna? *Terra Nova*, *13*(1), 25–31. https://doi.org/10.1046/j.1365-3121.2001.00301.x

D'Orazio, M., Innocenti, F., Tonarini, S., & Doglioni, C. (2007). Carbonatites in a subduction system: The Pleistocene alvikites from Mt. Vulture (southern Italy). *Lithos*, *98*(1-4), 313–334. https://doi.org/10.1016/j.lithos.2007.05.004

Faccenna, C., Becker, T. W., Lucente, F., Jolivet, L., & Rossetti, F. (2001). History of subduction and back-arc extension in the Central Mediterranean. *Geophysical Journal International*, *145*(3), 809–820. https://doi.org/10.1046/j.0956-540x.2001.01435.x

Faccenna, C., Civetta, L., d'Antonio, M., Funiciello, F., Margheriti, L., & Piromallo, C. (2005). Constraints on mantle circulation around the deforming Calabrian slab. *Geophysical Research Letters*, *32*, L06311. https://doi.org/10.1029/2004GL021874

Faccenna, C., Civetta, L., d'Antonio, M., Moroni, M., & Piromallo, C. (2007). *Slab disruption, mantle circulation, and the opening of the Tyrrhenian basins* (Special Paper No. 418). Geological Society of America.

Faccenna, C., Molin, P., Orecchio, B., Olivetti, V., Bellier, O., Funiciello, F., et al. (2011). Topography of the Calabria subduction zone (southern Italy): Clues for the origin of Mt. Etna. *Tectonics*, *30*, TC1003. https://doi.org/10.1029/2010TC002694

Frost, B. R., & Frost, C. D. (2019). Basalts and mantle structure. In *Essentials of igneous and metamorphic petrology* (pp. 82–89). Cambridge: Cambridge University Press. https://doi.org/10.1017/9781108685047.007

Gillot, P. Y., Kieffer, G., & Romano, R. (1994). The evolution of Mount Etna in the light of potassium-argon dating. *Acta Vulcanologica*, *5*, 81–87.

Glazner, A. F. (1991). Plutonism, oblique subduction, and continental growth: An example from the Mesozoic of California. *Geology*, *19*(8), 784–786. https://doi.org/10.1130/0091-7613(1991)019%3C0784:POSACG%3E2.3.CO;2

Goes, S., Giardini, D., Jenny, S., Hollenstein, C., Kahle, H.-G., & Geiger, A. (2004). A recent reorganization in the south-Central Mediterranean. *Earth and Planetary Science Letters*, *226*(3-4), 335–345. https://doi.org/10.1016/j.epsl.2004.07.038

Govers, R., & Wortel, M. J. R. (2005). Lithosphere tearing at STEP faults: Response to edges of subduction zones. *Earth and Planetary Science Letters*, *236*(1-2), 505–523. https://doi.org/10.1016/j.epsl.2005.03.022

Gudmundsson, A. (2003). Surface stresses associated with arrested dykes in rift zones. *Bulletin of Volcanology*, *65*(8), 606–619. https://doi.org/10.1007/s00445-003-0289-7

Gudmundsson, A. (2006). How local stresses control magma-chamber ruptures, dyke injections, and eruptions in composite volcanoes. *Earth-Science Reviews*, *79*(1-2), 1–31. https://doi.org/10.1016/j.earscirev.2006.06.006

Gudmundsson, A. (2011). *Rock fractures in geological processes*. Cambridge: Cambridge University Press. https://doi.org/10.1017/CBO9780511975684

Gutscher, M.-A., Dominguez, S., Mercier de Lepinay, B., Pinheiro, L., Gallais, F., Babonneau, N., et al. (2016). Tectonic expression of an active slab tear from high-resolution seismic and bathymetric data offshore Sicily (Ionian Sea). *Tectonics*, *35*, 39–54. https://doi.org/10.1002/2015TC003898

Gvirtzman, Z., & Nur, A. (1999). Formation of Mount Etna as a consequence of slab rollback. *Nature*, *401*(6755), 782–785. https://doi.org/10.1038/44555

Hamilton, W. B. (1995). Subduction systems and magmatism. In J. R. Smellie (Ed.), *Volcanism associated with extension to consuming plate margins*, *Special Publications* (Vol. 81, pp. 3–28). London: Geological Society.

Hirn, A., Nicolich, R., Gallart, J., & the ETNASEIS scientific Group (1997). Roots of Etna Volcano, faults of great earthquakes. *Earth and Planetary Science Letters*, *148*, 171–191.

Joron, J. L., & Treuil, M. (1984). Etude géochimique et pétrogenèse des laves de l'Etna. *Bulletin Volcanologique*, *47*(4), 1125–1144. https://doi.org/10.1007/BF01952368

Kostrov, V. V. (1974). Seismic moment and energy of earthquakes, and seismic flow of rock. *Physics of the Solid Earth*, *1*, 23–44.

Lanzafame, G., Neri, M., Coltelli, M., Lodato, L., & Rust, D. (1997). North-south compression in the Mt. Etna region (Sicily): Spatial and temporal distribution. *Acta Vulcanologica*, *9*, 121–133.

Lavecchia, G., Ferrarini, F., de Nardis, R., Visini, F., & Barbano, S. (2007). Active thrusting as a possible seismogenic source in Sicily (Southern Italy): Some insights from integrated structural-kinematic and seismological data. *Tectonophysics*, *445*(3-4), 145–167. https://doi.org/10.1016/j.tecto.2007.07.007

Le Maitre, R. W. (2002). *Igneous rocks. A classification and glossary of terms. Recommendations of the International Union of Geological Sciences Subcommission on the Systematics of Igneous Rocks*, 2nd, (xvi + 236). Cambridge, New York, Melbourne: Cambridge University Press.

Lentini, F., & Carbone, S. (2014). Geologia della Sicilia-Geology of Sicily. *Memorie Descrittive della Carta Geologica Italia*, *95*, 7–414.

Lundgren, P., Casu, F., Manzo, M., Pepe, A., Berardino, P., Sansosti, E., & Lanari, R. (2004). Gravity and magma induced spreading of Mount Etna volcano revealed by satellite radar interferometry. *Geophysical Research Letters*, *31*, L04602. https://doi.org/10.1029/2003GL018736

Marty, B., Trull, T., Lussiez, P., Basile, I., & Tanguy, J. (1994). He, Ar, O, Sr and Nd isotope constraints on the origin and evolution of Mt. Etna magmatism. *Earth and Planetary Science Letters*, *126*(1–3), 23–39. https://doi.org/10.1016/0012-821X(94)90240-2

Mastrolembo Ventura, B., Serpelloni, E., Argnani, A., Bonforte, A., Bürgmann, R., Anzidei, M. P., et al. (2014). Fast geodetic strain-rates in eastern Sicily (southern Italy): New insights into block tectonics and seismic potential in the area of the great 1693 earthquake. *Earth and Planetary Science Letters*, *404*, 77–88. https://doi.org/10.1016/j.epsl.2014.07.025

McDonough, W. F., & Sun, S. S. (1995). The composition of the Earth. *Chemical Geology*, *120*(3–4), 223–253. https://doi.org/10.1016/0009-2541(94)00140-4

Monaco, C., Bianca, M., Catalano, S., De Guidi, G., & Tortorici, L. (2002). Sudden change in the Late Quaternary tectonic regime in eastern Sicily: evidences from geological and geomorphological features. *Bollettino del Servizio geologico d'Italia*, *1*, 901–913.

Monaco, C., Catalano, S., Cocina, O., De Guidi, G., Ferlito, C., Gresta, S., et al. (2005). Tectonic control on the eruptive dynamics at Mt. Etna volcano (eastern Sicily during the 2001 and 2002-2003 eruptions). *Journal of Volcanology and Geothermal Research*, *144*, 221–233.

Monaco, C., Tapponier, P., Tortorici, L., & Gillot, P. Y. (1997). Late Quaternary slip rates on the Acireale-Piedimonte normal faults and tectonic origin of Mt. Etna (Sicily). *Earth and Planetary Science Letters*, *147*, 125–139.

Moran, S. C., Newhall, C., & Roman, D. C. (2011). Failed magmatic eruptions: Late-stage cessation of magma ascent. *Bulletin of Volcanology*, *73*, 115–122.

Morelli, C. (1997). The themes of crustal research in Italy and the role of the DSS-WA. *Seismics. Bollettino della Società Geologica Italiana*, *119*, 141–148.

Nakamura, K., & Uyeda, S. (1980). Stress gradient in arc-back arc regions and plate subduction. *Journal of Geophysical Research*, *85*(B11), 6419–6428. https://doi.org/10.1029/JB085iB11p06419

Neri, G., Orecchio, B., Totaro, C., Falcone, G., & Presti, D. (2009). Subduction beneath southern Italy Close the Ending: Results from seismic tomography. *Seismological Research Letters*, *80*, 63–70.

Nicotra, E., & Viccaro, M. (2012). Unusual magma storage conditions at Mt. Etna (southern Italy) as evidenced by plagioclase megacryst-bearing lavas: Implications for the plumbing system geometry and summit caldera collapse. *Bulletin of Volcanology*, *74*(4), 795–815. https://doi.org/10.1007/s00445-011-0566-9

Palano, M., Ferranti, L., Monaco, C., Mattia, M., Aloisi, M., Bruno, V., et al. (2012). GPS velocity and strain fields in Sicily and southern Calabria, Italy: Updated geodetic constraints on tectonic block interaction in the Central Mediterranean. *Journal of Geophysical Research*, *117*, B07401. https://doi.org/10.1029/2012JB009254

Patanè, D., Barberi, G., Cocina, O., de Gori, P., & Chiarabba, C. (2006). Time-resolved seismic tomography detects magma intrusions at Mount Etna. *Science*, *313*(5788), 821–823. https://doi.org/10.1126/science.1127724

Patanè, D., & Privitera, E. (2001). Seismicity related to 1989 and 1991–93 Mt. Etna (Italy) eruptions: Kinematic constraints by FPS analysis. *Journal of Volcanology and Geothermal Research*, *109*, 77–98.

Peccerillo, A. (2005). *Plio-Quaternary volcanism in Italy* (Vol. 365. pp. 1–370). New York: Springer Verlag Berlin Heidelberg.

Peccerillo, A. (2017). Cenozoic volcanism in the Tyrrhenian Sea region. In K. Nemeth (Ed.), *Advances in volcanology* (2nd ed., pp. 1–399). New York: Springer International Publishing. https://doi.org/10.1007/978-3-319-42491-0

Pedley, H. M., Debono, G., & Yeaman, M. (1993). Mesozoic structuring and volcanics along the Pelagian-Ionian boundary: A prelude to foundering of the Ionian basin. In M. D. Max & P. Colantoni (Eds.), *Geological development of the Sicilian-Tunisian platform* (Vol. 58, pp. 81–86). Paris: UNESCO.

Pondrelli, S. (2000). *European-Mediterranean regional centroid-moment tensors catalog* (RCMT) [data set]. Istituto Nazionale di Geofisica e Vulcanologia (INGV). https://doi.org/10.13127/rcmt/euromed

Puglisi, G., & Bonforte, A. (2004). Dynamics of Mount Etna volcano inferred from static and kinematic GPS measurements. *Journal of Geophysical Research*, *109*, B11404. https://doi.org/10.1029/2003JB002878

Ristuccia, G. M., Di Stefano, A., Gueli, A. M., Monaco, C., Stella, G., & Troja, S. O. (2013). OSL chronology of quaternary terraced deposits outcropping between Mt. Etna volcano and the Catania plain (Sicily, southern Italy). *Physics and Chemistry of the Earth*, *63*, 36–46. https://doi.org/10.1016/j.pce.2013.03.002

Rust, D., Behncke, B., Neri, M., & Ciocanel, A. (2005). Nested zones of instability in the Mount Etna volcanic edifice, Sicily. *Journal of Volcanology and Geothermal Research*, *155*, 137–153. https://doi.org/10.1016/j.jvolgeores.2004.11.021

Santo, A. P., Jacobsen, S. B., & Baker, J. (2004). Evolution and genesis of calc-alkaline magmas at Filicudi Volcano, Aeolian Arc (Southern Tyrrhenian Sea, Italy). *Lithos*, *72*(1–2), 73–96.

Savelli, C. (2002). Time-space distribution of magmatic activity in the western Mediterranean and peripheral orogens during the past 30 Ma (a stimulus to geodynamic considerations). *Journal of Geodynamics*, *34*(1), 99–126. https://doi.org/10.1016/S0264-3707(02)00026-1

Scarfì, L., Barberi, G., Barreca, G., Cannavo, F., Koulakov, I., & Patane, D. (2018). Slab narrowing in the Central Mediterranean: The Calabro-Ionian subduction zone as imaged by high resolution seismic tomography. *Scientific Reports*, *8*(5178). https://doi.org/10.1038/s41598-018-23543-8

Scarfì, L., Barberi, G., Musumeci, C., & Patane, D. (2016). Seismotectonics of northeastern Sicily and southern Calabria (Italy): New constraints on the tectonic structures featuring in a crucial sector for the Central Mediterranean geodynamics. *Tectonics*, *35*, 812–832. https://doi.org/10.1002/2015TC004022

Scarfì, L., Messina, A., & Cassisi, C. (2013). Sicily and southern Calabria focal mechanism database: A valuable tool for the local and regional stress field determination. *Annales de Geophysique*, *56*(1), D0109. https://doi.org/10.4401/ag-6109

Schiano, P., Clocchiatti, R., Ottolini, L., & Busa, T. (2001). Transition of Mount Etna lavas from a mantle-plume to an island-arc magmatic source. *Nature*, *412*(6850), 900–904. https://doi.org/10.1038/35091056

Schmincke, H. K., Behncke, B., Grasso, M., & Raffi, S. (1997). Evolution of the northwestern Hyblean Mountains, Sicily: Uplift, Pliocene/Pleistocene sea-level changes, paleoenviroment, and volcanism. *Geologische Rundschau*, *86*, 637–669.

Shen, Z. K., Jackson, D. D., & Ge, B. X. (1996). Crustal deformation across and beyond the Los Angeles basin from geodetic measurements. *Journal of Geophysical Research*, *101*(B12), 27,957–27,980.

Tanguy, J. C. (1987). Tholeitic basalt magmatism of Mount Etna and its relations with the alkaline series. *Contributions to Mineralogy and Petrology*, *66*, 51–67.

Tanguy, J. C., Condomines, M., & Kieffer, G. (1997). Evolution of the Mount Etna magma: Constraints on the present feeding system and eruptive mechanism. *Journal of Volcanology and Geothermal Research*, *75*(3-4), 221–250. https://doi.org/10.1016/S0377-0273(96)00065-0

Tibaldi, A. (2008). Contractional tectonics and magma paths in volcanoes. *Journal of Volcanology and Geothermal Research*, *176*(2), 291–301. https://doi.org/10.1016/j.jvolgeores.2008.04.008

Tibaldi, A. (2015). Structure of volcano plumbing systems: A review of multiparametric effects. *Journal of Volcanology and Geothermal Research*, *298*, 85–135. https://doi.org/10.1016/j.jvolgeores.2015.03.023

Tibaldi, A., Pasquarè, F., & Tormey, D. (2010). Volcanism in reverse and strike-slip fault settings. In S. Cloetingh & J. Negendank (Eds.), *New frontiers in integrated solid Earth sciences, international year of planet Earth* (pp. 315–348). New York: Science+Business Media B.V. https://doi.org/10.1007/978-90-481-2737-5_9

Tonarini, S., Armienti, P., D'Orazio, M., & Innocenti, F. (2001). Subduction-like fluids in the genesis of Mt. Etna magmas: Evidence from boron isotopes and fluid mobile elements. *Earth and Planetary Science Letters*, *192*, 471–483.

Torelli, L., Grasso, M., Mazzoldi, G., & Peis, D. (1998). Plio–quaternary tectonic evolution and structure of the Catania foredeep, the northern Hyblean Plateau and the Ionian shelf (SE Sicily). *Tectonophysics*, *298*(1-3), 209–221. https://doi.org/10.1016/S0040-1951(98)00185-1

Viccaro, M., Giacomoni, P. P., Ferlito, C., & Cristofolini, R. (2010). Dynamics of magma supply at Mt. Etna volcano (southern Italy) as revealed by textural and compositional features of plagioclase phenocrysts. *Lithos*, *116*(1-2), 77–91. https://doi.org/10.1016/j.lithos.2009.12.012

Walter, T. R., Acocella, V., Neri, M., & Amelung, F. (2005). Feedback processes between magmatic events and flank movement at Mount Etna (Italy) during the 2002–2003 eruption. *Journal of Geophysical Research*, *110*, B10205. https://doi.org/10.1029/2005JB003688

Ward, S. (1994). Constraints on the seismotectonics of the Central Mediterranean from very long baseline interferometry. *Geophysical Journal International*, *117*(2), 441–452. https://doi.org/10.1111/j.1365-246X.1994.tb03943.x

Wortel, M. J. R., & Spakman, W. (2000). Subduction and slab detachment in the Mediterranean-Carpathian region. *Science*, *290*(5498), 1910–1917. https://doi.org/10.1126/science.290.5498.1910

Yoder, H. S., & Tilley, C. E. (1962). Origin of basalt magmas: An experimental study of natural and synthetic rock systems. *Journal of Petrology*, *3*(3), 342–532. https://doi.org/10.1093/petrology/3.3.342

Zhang, H., Thurber, C., & Bedrosian, P. (2009). Joint inversion for *Vp*, *Vs*, and *Vp*/*Vs* at SAFOD, Parkfield, California. *Geochemistry, Geophysics, Geosystems*, *10*, Q110032. https://doi.org/10.1029/2009GC002709